

# Learning to Correspond Dynamical Systems

**Nam Hee Kim**

NHGK@CS.UBC.CA

**Zhaoming Xie**

ZXIE47@CS.UBC.CA

**Michiel van de Panne**

VAN@CS.UBC.CA

*2366 Main Mall #201, Vancouver, BC V6T 1Z4*

*Department of Computer Science, The University of British Columbia*

## Abstract

Correspondence across dynamical systems can lend us better tools for learning optimal control policies in new systems. We present a fully data-driven approach for putting multiple dynamical systems into correspondence. We utilize symmetric nearest neighbor distances in our loss function to encourage states of different sources to reside in close proximity in a shared latent state space. We also construct and enforce a dynamics in the latent space, which helps avoid temporal ambiguity of state projections. We demonstrate the effectiveness of our approach by putting a 2D walker character into correspondence with a PD-controlled pendulum and with a 2D walker character with a different morphology.

**Keywords:** dynamical correspondence, latent dynamics, autoencoders

## 1. Introduction

Naturally occurring movement patterns such as locomotion are inherently similar across different species (Alexander and Jayes, 1983). For example, although a human and an ostrich have very different anatomical features, both share a fundamental system of joints that work together to produce bipedal gaits. In principle, knowing the similarities across these bipedal locomotion patterns should be beneficial for building a controller for a new bipedal robot. More generally, encapsulating the similarities across dynamical systems can improve the learning of optimal control policies in new systems. Correspondence is a well-established framework for extracting and examining such similarities. Despite this promising direction, there have been relatively little literature examining methods to learn the correspondence across multiple dynamical systems.

In this paper, we introduce a simple supervised learning method named L2CDS (Learning to Correspond Dynamical Systems). To the best of our knowledge, L2CDS is the first fully data-driven approach that can put two or more dynamical systems into correspondence by extracting a shared latent state space that encapsulates the similarities across the motions of the systems. Using this method, one can project between a source system’s state to a target system’s state by encoding onto the latent space and then decoding onto the target state space.

Our main contributions are as follows. First, we formalize the problem of dynamical system correspondence and introduce a latent space learning approach to solving it in a modular fashion. Next, we introduce an autoencoder-based deep learning architecture that finds the correspondence across the states of two or more dynamical systems. Finally, we correspond several different well-studied systems used in dynamic control and evaluate their correspondence both qualitatively and quantitatively.

For qualitative results and visual intuition, we refer the reader to the supplementary video, which is available in the following URL: <https://youtu.be/f64hhir6lV8>.

## 2. Related Work

**Correspondence** Correspondence is a class of problems where similar features across multiple systems are aligned together. One may view correspondence as a matching between different modalities of a common latent object. Shape correspondence has been well studied in the computer graphics literature. Iterative closest point (ICP) (Besl and McKay, 1992) is a classical method to solve shape correspondence. There are also significant work on motion retargeting, where kinematic sequences are transferred between characters with different morphologies, e.g. (Jain and Liu, 2011) (Rhodin et al., 2014). Relatively few works deal with correspondence in dynamical systems, which is the focus of our work.

**Template models for locomotion** Due to the high degrees of freedom for a typical biped, simplified models are often used to simplify the modeling and control of these dynamical systems. Most popular ones include linear inverted pendulum (Kajita et al., 2001), inverted pendulum (Pratt et al., 2006) and spring loaded inverted pendulum (Geyer et al., 2006). These models and the variants of them are utilized to design simple control laws for the original complicated bipedal systems. Robots of different morphologies are also corresponded together to simplify control design. For example, Raibert (1986) use correspondences between one-legged hopper, biped and quadruped gait to design locomotion policies for them. The aforementioned methods involve hand-crafting the reduction from a complex system to a simpler system with lower degrees of freedom. Instead, our work focuses on leveraging state trajectory data to learn the reduction using autoencoder modules.

**Autoencoders with latent dynamics** Learning the dynamics of the motion and the physical environment is a classic learning problem in the control literature. Early arguments for learned dynamics can be traced to the 1980s, e.g. (Werbos, 1987). Watter et al. (2015) instead learned the dynamics on the latent space produced via variational autoencoders and demonstrated that the latent dynamics can be utilized for easier control. Ha and Schmidhuber (2018) proposed using learned latent dynamics to augment reinforcement learning. More recently, Hafner et al. (2019) used the latent system exclusively to learn the control policy of the original system. Our work concerns using latent dynamics as a mechanism to achieve correspondence with temporal consistency, as to aid the correspondence of dynamical systems. Our eventual aim is to leverage the learned latent dynamics to improve efficiency and stability of reinforcement learning in continuous control.

## 3. Method

### 3.1. Problem Formulation

In this paper, we only consider discrete-time dynamical systems. A discrete-time dynamical system consists of a tuple  $(\mathcal{S}, f)$ , with the state space  $\mathcal{S} \subseteq \mathbb{R}^n$  and the transition function  $f : \mathcal{S} \rightarrow \mathcal{S}$ . The state of the dynamical system  $s_{t+1}$  at time  $t + 1$  can be computed from the state  $s_t$  at time  $t$  via  $s_{t+1} = f(s_t)$ .

Given two dynamical systems  $A = (\mathcal{S}^A, f^A)$  and  $B = (\mathcal{S}^B, f^B)$ , our goal is to find a pair of correspondence functions  $C_A^B : \mathcal{S}^A \rightarrow \mathcal{S}^B$  and  $C_B^A : \mathcal{S}^B \rightarrow \mathcal{S}^A$ .  $C_A^B$  projects a state of the source system  $A$  to the state space of the target system  $B$ .  $C_B^A$  is the inverse of  $C_A^B$ . The correspondence functions must not only map the distributions of states, but also honor the temporal ordering of states based on each system’s dynamics:

$$C_A^B(s_{t+1}^A) = f^B(C_A^B(s_t^A)), \quad C_B^A(s_{t+1}^B) = f^A(C_B^A(s_t^B)). \quad (1)$$

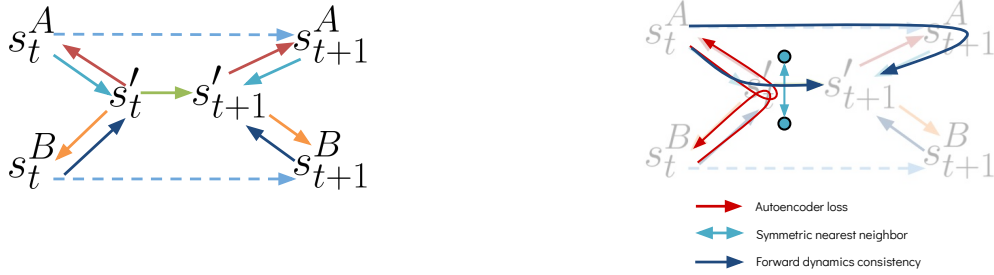


Figure 1: Left: summary figure for variables and mappings in L2CDS, where each solid arrow represents a machine learning model. Dotted arrows represent the forward dynamics of original state trajectories. Right: summary figure of losses involved in optimizing L2CDS. Traversing the arrows in the left figure results in backpropagation-enabled transformations. Best viewed in color.

In other words, consecutive states in the original system must correspond to consecutive states in the target system.

### 3.2. Latent Dynamical System

Instead of directly learning the corresponding function  $C_A^B$ , we embed the two dynamical systems into a latent dynamical system  $D' = (S', f')$ . More formally, we first learn the correspondence function  $C_A^{D'}$  and  $C_{D'}^B$ , and then compose the two functions  $C_A^{D'} \circ C_{D'}^B$ , to compute  $C_A^B$ . See Figure 1 for a graphical representation of this approach. Note that the latent dynamical system does not come for free and we need to construct  $S'$  and  $f'$  via learning as well. Learning a latent space has a few major benefits over learning the correspondence functions directly. First, learning the latent space yields more flexibility to utilize the latent state distribution and dynamics. These components can represent a latent system which can be simulated on its own. Next, the latent space encapsulates similarity across the source and target systems, and thus learning the latent space can replace analytical reductions (e.g. inverted pendulum (Geyer et al., 2006)) while preserving interpretability. Finally, in case more than two systems are put into correspondence, the overall mappings can be constructed in a bottom-up fashion, where each system only need to learn the embedding onto the existing latent space. This can greatly improve the scalability of correspondence learning.

### 3.3. Collecting State Trajectories

To learn the correspondence functions in a data-driven fashion, we rely on the collection of state trajectories for each system of interest. For systems A and B, we compile datasets  $\mathcal{D}^A$  and  $\mathcal{D}^B$  by simulating each system forward. We advance each state trajectory to a desired horizon and then restart the system with some randomness to collect a new one. More formally:

$$\mathcal{D} = \bigcup_{i=1}^R \{ \langle s_t, s_{t+1} \rangle \mid t = 1, 2, \dots, H \}_i \quad (2)$$

where  $i$  is the state trajectory index,  $H$  is the horizon for each trajectory, and  $R$  is the number of resets performed during collection. The same data collection strategy is used for systems A and B.

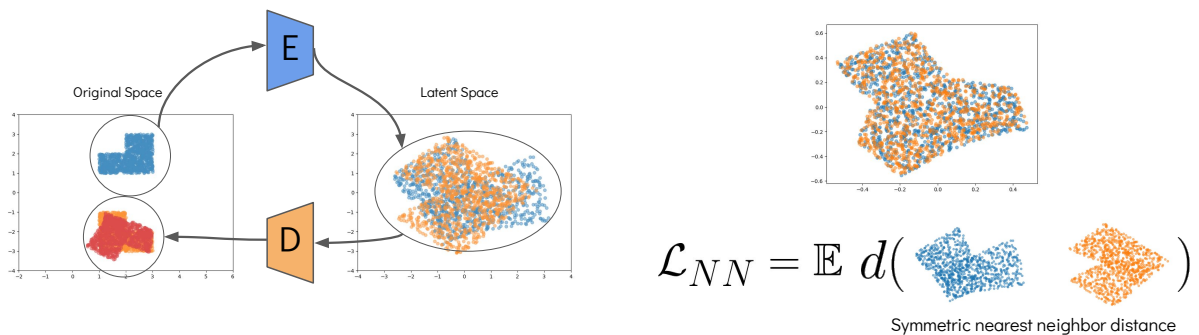


Figure 2: Left: naïvely learned autoencoders do not enforce latent space to be shared across systems. Right: regularizing for the minimum distance between the two sets of latent space can act to fuse state distributions together. Best viewed in color.

### 3.4. Autoencoders

We employ autoencoders (Kramer, 1991) to project original states onto the latent state space and then back onto the original state space ( $s_t \rightarrow s'_t \rightarrow \hat{s}'_t$ ). To use the terminology of autoencoders, we denote the corresponding function and its inverse to be  $E$  (encoder) and  $D$  (decoder) respectively. One can project a state in the original space onto the latent space and/or project a latent state onto the original space with the following set of operations:

$$s_t'^A = E^A(s_t^A) \quad \hat{s}_t^A = D^A(s_t'^A) \quad s_t'^B = E^B(s_t^B) \quad \hat{s}_t^B = D^B(s_t'^B) \quad (3)$$

Where  $E^A$  and  $D^A$  are the encoder and the decoder for the states of system A, and so on. Note that the arguments for decoders  $D^A$  and  $D^B$  are interchangeable, since latent states  $s_t'^A$  and  $s_t'^B$  share the same space. Reconstructed states  $\hat{s}_t^A$  and  $\hat{s}_t^B$  are used as the corresponded states at the tail-end of our pipeline. To ensure that the reconstructed state is consistent with the original state, we use the autoencoder loss (Note that states  $s_t^A$  and  $s_t^B$  are sampled from datasets  $\mathcal{D}^A$  and  $\mathcal{D}^B$ , not decoders):

$$\mathcal{L}_{AE}(\mathcal{D}) = \mathbb{E}_{s_t^A \sim \mathcal{D}^A, s_t^B \sim \mathcal{D}^B} [\| \hat{s}_t^A - s_t^A \|^2 + \| \hat{s}_t^B - s_t^B \|^2] \quad (4)$$

One may recognize this as a cycle consistency loss as often used in the generative adversarial networks framework (Zhu et al., 2017).

### 3.5. Symmetric Nearest Neighbors

When an encoder-decoder pair is learned for each system, the encoders are not constrained to produce overlapping latent state distributions across the systems of interest. This prohibits using decoders interchangeably for correspondence (see Figure 2). We employ a symmetric nearest neighbor loss, where the encoders are penalized for mapping onto subspaces far away from other encoders.

For our 2-system example, the nearest neighbors loss is computed by (1) sampling a separate batch from each dataset, i.e.  $s_t^A \sim \mathcal{D}^A$  and  $s_t^B \sim \mathcal{D}^B$ , (2) computing latent states  $s_t'^A$  and  $s_t'^B$  for each batch, and (3) computing the minimum distance between each state in system A and another state in system B, and vice versa. We minimize the expected minimum distances by introducing the

following loss term:

$$\mathcal{L}_{NN}(\mathcal{D}) = \mathbb{E}_{s_t^A \sim \mathcal{D}^A, s_t^B \sim \mathcal{D}^B} \left[ \min_{s_t^B} \|s_t^A - s_t^B\|^2 + \min_{s_t^A} \|s_t^A - s_t^B\|^2 \right] \quad (5)$$

Figure 2 illustrates the effect of this loss function.

### 3.6. Latent Forward Dynamics

Up to this point, we have enforced different systems to project their states onto the same latent state space and required latent states of different sources to reside in close proximity. However, although the previous loss terms enforce spatial consistency in latent state distribution, the resulting temporal ordering of the latent states is highly ambiguous, without the dynamics constraint as required by Equation 1. We prevent this degeneracy by introducing a latent dynamics model that is shared across the systems of interest. The latent dynamics model  $F$  takes a latent state and produces a displacement to the latent state at next time step:

$$v'_t = F(s'_t), \quad s'_{t+1} = s'_t + v'_t. \quad (6)$$

We encourage the encoder to project states  $s_t$  and  $s_{t+1}$  to the latent state space and ensure that the encoder’s results are consistent with the latent dynamics. The following loss function expresses this objective:

$$\mathcal{L}_{FD}(\mathcal{D}) = \mathbb{E}_{(s_t, s_{t+1}) \sim \mathcal{D}} [\| (s'_t + F(s'_t)) - s'_{t+1} \|^2]. \quad (7)$$

Note that the latent forward dynamics model  $F$  is learned in a fully unsupervised fashion, essentially providing regularization for  $\mathcal{L}_{FD}$ . We still optimize  $F$  along with other modules such that its predictions are stable.

Furthermore, a state in a Markovian dynamical system must describe all information necessary for predicting the next timestep. Practically, a state  $s_t$  typically breaks down into the pose  $\theta_t$  and the velocity  $\dot{\theta}_t$  of the system. Then the dynamics function establishes a differential equation involving  $\theta_t$ ,  $\dot{\theta}_t$ , and  $\ddot{\theta}_t$  (acceleration) of the system. We reflect this in the latent space, so that the latent system also honors the Markovian definition of a state. In other words, we encourage the encoders to produce latent states that observe the relationship between position and velocity with respect to time. More formally, let

$$\begin{bmatrix} \theta'_t \\ \dot{\theta}'_t \end{bmatrix} = s'_t, \quad \begin{bmatrix} \theta'_{t+1} \\ \dot{\theta}'_{t+1} \end{bmatrix} = s'_{t+1} \quad (8)$$

where  $\theta'_t$  and  $\dot{\theta}'_t$  are the pose and the velocity of the latent system at time  $t$ , respectively. If  $|s'_t| = 2k$ , then  $|\theta'_t| = |\dot{\theta}'_t| = k$ . We minimize the following loss:

$$\mathcal{L}_{PV}(\mathcal{D}) = \mathbb{E}_{(s_t, s_{t+1}) \sim \mathcal{D}} [\| (\theta'_t + \dot{\theta}'_t) - \theta'_{t+1} \|^2] \quad (9)$$

to encourage the encoders to find the subspace within the latent space that honors the pose-velocity relationship.

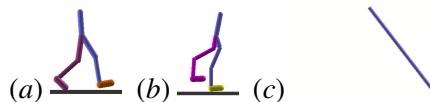


Figure 3: (a) `walker2d`: a 2D walker character with 6 joints.  $|s_t| = 17$ . (b) `ostrich2d`: a slightly taller 2D walker character with 8 joints.  $|s_t| = 21$ . (c) `pendulum`: a classic 1-DOF pendulum system driven by a PD controller.

### 3.7. Final Loss Function and Runtime Procedure

Our final loss function is the weighted sum of the four loss functions introduced above:

$$\mathcal{L}(\mathcal{D}) = \lambda_{AE}\mathcal{L}_{AE}(\mathcal{D}) + \lambda_{NN}\mathcal{L}_{NN}(\mathcal{D}) + \lambda_{FD}\mathcal{L}_{FD}(\mathcal{D}) + \lambda_{PV}\mathcal{L}_{PV}(\mathcal{D}) \quad (10)$$

where loss weights  $\lambda_{AE}$ ,  $\lambda_{NN}$ ,  $\lambda_{PV}$ , and  $\lambda_{FD}$  are selected experimentally so that the resulting correspondence is qualitatively and quantitatively sound.

After training, correspondence is achieved by using the learned mappings to project source system states to the latent space, and then projecting the latent states to the target system state space. In other words, we can put states into correspondence by using the learned decoders interchangeably.

## 4. Experiments

Figure 3 shows the three systems we use for our experiments. We put these systems into correspondence using the L2CDS pipeline. These systems are simulated with DART (Lee et al., 2018). The neural networks and learning algorithms are implemented in PyTorch (Steiner et al., 2019). RAdam (Liu et al., 2019) is used to optimize the neural network parameters. We use  $256 \times 256$  multi-layer perceptrons (MLPs), where ReLU is used as hidden layer activation and Tanh is applied at the final output to limit the output range. We use a batch size of 4096 for stochastic gradient descent; note that this is high compared to what is typically used for other learning tasks but is necessary in our settings to accommodate for sampling accuracy in symmetric nearest neighbors loss. To prevent state decoders and forward dynamics models from learning to separate latent states of different sources, we add a small amount of Gaussian noise to the inputs of the decoder networks and the latent forward dynamics model. The effect of the noise is significant, as summarized in Table 1.

The dynamical systems we consider also have control input involved. To make the dynamical systems fully autonomous, we pre-train a policy for each system. In particular, the pendulum is running a PD controller that tracks a time-varying PD target that repeats at a fixed period, `walker2d` and `ostrich2d` run policies that track repeating walking cycles, which are obtained using DeepMimic (Peng et al., 2018). This introduces an additional “phase” variable  $\phi$ , into the state of these systems, where  $\phi_{t+1} = (\phi_t + 1) \bmod P$ ,  $P$  being the period of the motion regardless of other state variables. Note that each dynamical system forms a stable limit cycle, i.e., starting from any state, the trajectories will converge to the limit cycle. We opted to take advantage of the phase variable and use it as an input to our latent forward dynamics model.

When generating the state trajectories, we add small random noise  $\epsilon \sim \mathcal{N}(0, \sigma^2)$  to the policies, as to encourage more variety in states visited. To eliminate the influence of the made up phase variable, we remove the phase from the states when we put them through the state encoders, but we still use the phase when we train our latent dynamics.

Quantitatively, we evaluate the correspondence by measuring the difference between the distributions of the original states  $s_t$  and the reconstructed states  $\hat{s}_t$  after using the learned projections in L2CDS ( $s_t \rightarrow s'_t \rightarrow \hat{s}_t$ ). As a heuristic to this difference, we use the mean symmetric nearest neighbor (MSNN) distances within the original state space:

$$\mathcal{E}_{MSNN} = \frac{1}{2n} \left( \sum_{s_t} \min_{\hat{s}_t} \|s_t - \hat{s}_t\| + \sum_{\hat{s}_t} \min_{s_t} \|s_t - \hat{s}_t\| \right) \quad (11)$$

where  $n$  is the number of states stored in the dataset.

Qualitatively, we observe similarities in corresponding states of different systems. Namely, we simulate one character with the pre-trained policy and use the learned mappings to generate the corresponding states of another system. We particularly focus on the effect of perturbations in the simulated system. A good correspondence across dynamical systems must take into account the system’s interactions with its physical environment, such as contact and forces. Therefore, we expect the correspondence to go beyond a simple mapping between multiple limit cycles; rather, the dynamics must capture and put perturbed states of systems into correspondence.

#### 4.1. Corresponding 2D Walker with Pendulum

Our method successfully learns to correspond the classical 2D walker character with the pendulum. The supplementary video shows that the swing of the pendulum is aligned with gait of the walker, such that one swing of the pendulum completes as one walking cycle of the walker is completed. The limit cycle drawn with the estimated corresponding states of the pendulum shows that both the position and the velocity of the pendulum are reconstructed with high precision. Finally, perturbing the walker with an external force results in the perturbation of the pendulum, showing that the state-to-state mapping goes beyond a simple matching of two cycles.

#### 4.2. Corresponding 2D Walkers

##### 4.2.1. ANALYSIS OF REPORTED ERRORS

Table 1 shows  $\mathcal{E}_{MSNN}$  computed on various configurations on the walker-ostrich correspondence case. We ablate each logical component of the full loss function and also show the impact of the presence of noise in the inputs of state decoders and forward dynamics models. We use Equation 11 on a test dataset of  $n = 1000$  state tuples, generated with a random seed different from that of the training data (otherwise exact same procedure).

In Table 1, WLW (walker-latent-walker) and OLO (ostrich-latent-ostrich) are the two projections that consistently achieve low  $\mathcal{E}_{MSNN}$ . This is granted since state reconstruction in these two projections is directly correlated with the autoencoder loss  $\mathcal{L}_{AE}$  in Equation 4. Once the inter-system correspondence is involved (i.e. WLWL, OLWLO, WLO, OLW),  $\mathcal{E}_{MSNN}$  increases as the latent state distributions are no longer identical. Without  $\mathcal{L}_{NN}$ , the model can achieve a very low  $\mathcal{E}_{MSNN}$  for WLW and OLO, but the latent states of different sources are far apart, making the error very high for other projections.

The lowest  $\mathcal{E}_{MSNN}$  involving inter-system correspondence is achieved by learning the model without the latent forward dynamics components. However, visualizing the results, we see that this model yields a qualitatively poor correspondence, due to the ambiguities induced by the lack of

		WLW	OLO	WLWLW	OLWLO	WLO	OLW
Without noise	Full model	2.76	6.48	7.28	13.08	6.43	6.64
	Without $\mathcal{L}_{FD}, \mathcal{L}_{PV}$	0.74	0.97	1.01	1.31	5.67	4.78
	Without $\mathcal{L}_{NN}$	1.09	1.33	52.87	89.24	39.90	95.61
With noise	Full model	1.04	1.37	1.43	2.07	5.61	5.13
	Without $\mathcal{L}_{FD}, \mathcal{L}_{PV}$	0.64	0.90	0.91	1.17	5.64	4.71
	Without $\mathcal{L}_{NN}$	1.05	1.37	22.79	49.56	16.79	23.79

Table 1: Mean Symmetric Nearest Neighbor (MSNN) distances for walker-ostrich correspondence case. W=Walker, L=Latent, O=Ostrich. WLW refers to using learned mappings to project walker-latent-walker ( $s_t^{\text{walker}} \rightarrow s'_t \rightarrow \hat{s}_t^{\text{walker}}$ ), and so on. “Noise” refers to Gaussian noise being added to each decoder and the latent forward dynamics model.

temporal consistency in the latent states. On the other hand, adding some noise to state decoders and the latent forward dynamics model has a significant effect on the reduction of  $\mathcal{E}_{MSNN}$ . This is thanks to state encoders producing latent states that state decoders and forward dynamics models cannot distinguish, encouraging a homogeneous mixture of the latent states of different sources. We note that the full model with noise achieves the next best performance in terms of  $\mathcal{E}_{MSNN}$ , and has the most qualitatively sound result. For the qualitative results of this ablation study, we refer the reader to the supplementary video.

#### 4.2.2. ARE THE PERTURBED STATE MAPPINGS MEANINGFUL?

As mentioned, a true correspondence between dynamical systems must go beyond a simple mapping between two periodic trajectories. Examining perturbations is therefore crucial in assessing the validity of our method. We provide a brief statistical analysis to show that the perturbed states indeed map to each other in a meaningful way. To this end, we use the correlation between the original system’s root x-velocity and the corresponded root x-velocity of the target system. We prepare simple linear models:

$$\hat{x}_t^B \sim \beta \dot{x}_t^A + \epsilon \quad (12)$$

$$\hat{x}_t^B \sim \beta_0 + \beta_1 \dot{x}_t^A + \epsilon \quad (13)$$

where  $\dot{x}_t^A \in s_t^A$  and  $\hat{x}_t^B \in \hat{s}_t^B$  are the root x-velocity of system A and the estimated corresponding system B state. We first sample  $s_t^A$  from the state trajectory dataset. For each  $s_t^A$ , we generate 10 new data points by adding a uniform noise to  $\dot{x}_t^A$  to create diverse scenarios where the root x-velocity is perturbed. We then predict  $\hat{s}_t^B$  using L2CDS and finally learn the regression coefficients  $\beta$ ,  $\beta_0$ , and  $\beta_1$ .

Figure 4 summarizes the results of the above experiment on the  $n = 1000$  states gathered from `ostrich2d` and `walker2d`. In both OLW and WLO, the slope coefficient of the simple linear model is significantly above zero with the reported  $p \ll 0.05$ , whether the intercept is included or not. This shows that perturbations such as a forward or backward push on the original system results in a push in the same direction on the target system when L2CDS is used to estimate the corresponding target system states.



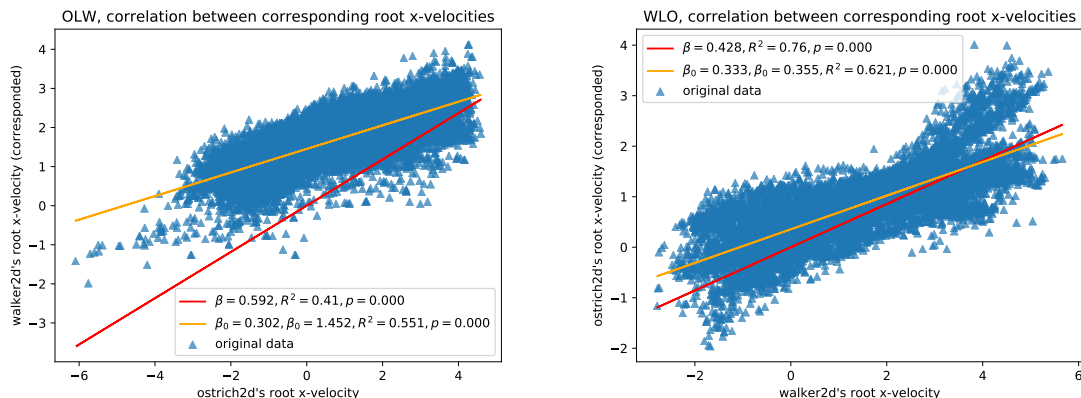


Figure 4: Results of linear regression on the corresponded root x-velocity vs. the source system’s root x-velocity. The lines represent the learned linear models.  $\beta$ ,  $\beta_0$ ,  $\beta_1$  correspond to the parameters specified in Equations 12 and 13. Red: without intercept. Orange: with intercept. Best viewed in color.

## 5. Discussion

In this paper, we presented L2CDS, a fully data-driven method that can learn the correspondence across the states of two or more dynamical systems. L2CDS achieves correspondence by viewing the input systems as different modalities of a common latent system. This latent system is modeled by learning the latent state space and the latent dynamics simultaneously based on the state trajectory data.

### 5.1. Limitations

In our experiments, the scope is limited to examining the correspondence across discrete-time Markovian dynamical systems. Moreover, each physics-simulated character (`walker2d`, `ostrich2d`, `pendulum`) was designed to complete its limit cycle in a fixed number of timesteps, and thus the resulting corresponding state trajectories can align perfectly. In real systems, however, it is difficult to expect such a perfect alignment due to the high levels of noise. Note that although the experiments are mainly concerning periodic systems, the method can apply to aperiodic systems in principle.

### 5.2. Future Work

This work provides a promising proof of concept that a latent dynamical system can be learned to canonize the dynamics functions of multiple different systems. A natural extension of this work is to leverage the canonical dynamics, i.e. the latent dynamics learned across two or more dynamical systems, in place of hand-crafted reductions such as the inverted pendulum in bipedal locomotion. In principle, the canonical dynamics encapsulates the observable similarities across the input systems and thus can generalize to other novel but similar systems. Therefore, learning the control policy for a novel but similar system may only require learning its correspondence with the latent system

following the canonical dynamics. This is a promising direction for achieving a more efficient and stable learning through knowledge transfer where an agent can learn by analogy.

## References

- R McN Alexander and AS Jayes. A dynamic similarity hypothesis for the gaits of quadrupedal mammals. *Journal of zoology*, 201(1):135–152, 1983.
- Paul J Besl and Neil D McKay. Method for registration of 3-d shapes. In *Sensor fusion IV: control paradigms and data structures*, volume 1611, pages 586–606. International Society for Optics and Photonics, 1992.
- Hartmut Geyer, Andre Seyfarth, and Reinhard Blickhan. Compliant leg behaviour explains basic dynamics of walking and running. *Proceedings of the Royal Society B: Biological Sciences*, 273(1603):2861–2867, 2006.
- David Ha and Jürgen Schmidhuber. World models. *arXiv preprint arXiv:1803.10122*, 2018.
- Danijar Hafner, Timothy Lillicrap, Jimmy Ba, and Mohammad Norouzi. Dream to control: Learning behaviors by latent imagination, 2019.
- Sumit Jain and C. Karen Liu. Motion analogies : Automatic motion transfer to different morphologies. 2011.
- Shuuji Kajita, Fumio Kanehiro, Kenji Kaneko, Kazuhito Yokoi, and Hirohisa Hirukawa. The 3d linear inverted pendulum mode: A simple modeling for a biped walking pattern generation. In *Proceedings 2001 IEEE/RSJ International Conference on Intelligent Robots and Systems. Expanding the Societal Role of Robotics in the the Next Millennium (Cat. No. 01CH37180)*, volume 1, pages 239–246. IEEE, 2001.
- Mark A Kramer. Nonlinear principal component analysis using autoassociative neural networks. *AICHE journal*, 37(2):233–243, 1991.
- Jeongseok Lee, Michael X Grey, Sehoon Ha, Tobias Kunz, Sumit Jain, Yuting Ye, Siddhartha S Srinivasa, Mike Stilman, and C Karen Liu. Dart: Dynamic animation and robotics toolkit. *J. Open Source Software*, 3(22):500, 2018.
- Liyuan Liu, Haoming Jiang, Pengcheng He, Weizhu Chen, Xiaodong Liu, Jianfeng Gao, and Jiawei Han. On the variance of the adaptive learning rate and beyond, 2019.
- Xue Bin Peng, Pieter Abbeel, Sergey Levine, and Michiel van de Panne. Deepmimic: Example-guided deep reinforcement learning of physics-based character skills. *ACM Trans. Graph.*, 37(4):143:1–143:14, July 2018. ISSN 0730-0301. doi: 10.1145/3197517.3201311. URL <http://doi.acm.org/10.1145/3197517.3201311>.
- Jerry Pratt, John Carff, Sergey Drakunov, and Ambarish Goswami. Capture point: A step toward humanoid push recovery. In *2006 6th IEEE-RAS international conference on humanoid robots*, pages 200–207. IEEE, 2006.

- Marc H. Raibert. *Legged Robots That Balance*. Massachusetts Institute of Technology, Cambridge, MA, USA, 1986. ISBN 0-262-18117-7.
- Helge Rhodin, James Tompkin, Kwang In Kim, Varanasi Kiran, Hans-Peter Seidel, and Christian Theobalt. Interactive motion mapping for real-time character control. *Computer Graphics Forum (Proceedings Eurographics)*, 33(2), 2014.
- Benoit Steiner, Zachary DeVito, Soumith Chintala, Sam Gross, Adam Paszke, Francisco Massa, Adam Lerer, Gregory Chanan, Zeming Lin, Edward Yang, et al. Pytorch: An imperative style, high-performance deep learning library. *Advances in Neural Information Processing Systems*, 32, 2019.
- Manuel Watter, Jost Springenberg, Joschka Boedecker, and Martin Riedmiller. Embed to control: A locally linear latent dynamics model for control from raw images. In *Advances in neural information processing systems*, pages 2746–2754, 2015.
- Paul J Werbos. Learning how the world works: Specifications for predictive networks in robots and brains. In *Proceedings of IEEE International Conference on Systems, Man and Cybernetics, NY*, 1987.
- Jun-Yan Zhu, Taesung Park, Phillip Isola, and Alexei A Efros. Unpaired image-to-image translation using cycle-consistent adversarial networks. In *Proceedings of the IEEE international conference on computer vision*, pages 2223–2232, 2017.